Linear and stable photonic radio frequency phase shifter based on a dual-parallel Mach–Zehnder modulator using a two-drive scheme

Jianguo Shen,[1,2] Guiling Wu,[1,*] Weiwen Zou,[1] Ruihao Chen,[1] and Jianping Chen[1]

[1]State Key Laboratory of Advanced Optical Communication Systems and Networks, Department of Electronic Engineering, Shanghai Jiao Tong University, Shanghai 200240, China

[2]College of Mathematics, Physics and Information Engineering, Zhejiang Normal University, Jinhua, Zhejiang 321004, China

*Corresponding author: wuguiling@sjtu.edu.cn

Received 12 August 2013; revised 20 October 2013; accepted 28 October 2013; posted 29 October 2013 (Doc. ID 195593); published 25 November 2013

We theoretically and experimentally demonstrate a linear and stable photonic RF phase shifter based on a dual-parallel Mach–Zehnder modulator (DPMZM) using a two-drive scheme. To avoid the effect of the residual optical carrier and overcome the lowest frequency limit from the optical filter, a local microwave signal and a signal up-converted from the under-phase-shifted RF signal are applied to the two RF inputs of the DPMZM, respectively. A phase-shifted RF signal is generated by beating the two first-order upper sidebands located in the passband of the optical filter. A continuous and linear phase shift of more than 360° and power variation of less than ±0.15 dB at 1 GHz are achieved by simply tuning the bias voltage of the modulator. A phase tuning bandwidth of more than 17 MHz and phase drift of less than 0.5° within 2000 s are also observed.

OCIS codes: (060.5625) Radio frequency photonics; (060.5060) Phase modulation.
http://dx.doi.org/10.1364/AO.52.008332

1. Introduction

Photonic RF phase shifters have attracted a growing research interest in past decades due to their potential application in phased array beam-forming, ultrahigh-speed signal processing, and microwave photonic filters [1–3]. Compared to their electrical counterparts, they have the advantage of wide bandwidth, large tunable range, and immunity to electromagnetic interferences. Up to date, various schemes of photonic RF phase shifters based on vector sum [4], heterodyne mixing [5,6], stimulated Brillouin scattering effect in optical fibers [7,8], slow and fast light effect in semiconductor optical amplifier [9], and cross-phase modulation in a nonlinear optical-loop mirror [10] have been proposed. However, the performance of these schemes in terms of linearity, stability, and system complexity is still limited for many practical applications. A linear photonic RF phase shifter based on the polarization sensitive effect of optical phase modulators has been demonstrated, which can achieve a continuous phase shift of more than 360° by simply tuning the DC voltage of the phase modulator [11,12]. This kind of phase shifters, however, cannot work at wideband microwave signals.

Recently, Pan and Zhang [13] proposed a wideband photonic phase shifter based on a single sideband polarization modulator and a polarizer, which can achieve a power variation of less than ±0.5 dB within a phase shift over 360°. We proposed another wideband and near-linear photonic RF phase shifter based on a dual-parallel Mach–Zehnder modulator

1559-128X/13/348332-06$15.00/0

(DPMZM) and an optical filter using a single-drive scheme [14]. The scheme makes the system simpler and stable by generating and phase-shifting two optical subcarriers (optical carrier and the upper sideband) in a single DPMZM simultaneously. However, there still exists some nonlinearity and power variation induced by the residual optical carrier owing to the finite extinction ratio of the modulator. Moreover, the lowest work frequency of the proposed phase shifter is limited by the smallest transition bandwidth of the available optical filters.

In this paper, we proposed a DPMZM based photonic RF phase shifter using a two-drive scheme, which can improve the nonlinearity and power variation induced by the residual optical carrier and overcome the lowest frequency limit from the optical filter. In the proposed scheme, the two RF inputs of the DPMZM are driven by a local microwave signal and a signal up-converted from the under-phase-shifted RF signal with the assistant of the local microwave signal, respectively. The two first-order upper sidebands generated by the two drives are selected by an optical filter to generate the phase-shifted RF signal. Since the two first-order modulation sidebands are independent of the extinction ratio of the modulator and can be filtered easily by the optical bandpass filter (OBPF) by selecting the suitable frequency of the local microwave signal, the linearity and stability of the proposed phase shifter can be improved and its lowest limit of work frequency can be extended. A continuous and linear phase shift over 360° and power variation of less than ±0.15 dB at 1 GHz are experimentally achieved by simply tuning the bias voltage of the DPMZM. The phase-tuning bandwidth and phase drift of the proposed phase shifter are also presented.

2. Principle

The schematic of the proposed photonic RF phase shifter is shown in Fig. 1. The CW light wave from a frequency stabilized laser with low relative intensity noise is launched into an integrated x-cut DPMZM composed of two parallel sub-MZMs, respectively, lying on two arms of the parent MZM. A local microwave signal is split into two branches. One is injected into the RF input port on the top arm of the DPMZM directly; the other one is sent to an electric up-converter (U-C) to assist the up-conversion of the under-phase-shifted RF signal. The up-converted signal is applied to the RF input port on the bottom arm of the DPMZM. The bias voltage of DC1 and DC2 are optimally biased at the minimum transmission point in order to perform optical carrier-suppressed double sideband (CS-DSB) modulation. The first-order sidebands in the same side of two CS-DSB signals are selected by an OBPF to produce a phase-shifted RF signal on the photo detector (PD). The phase shift of the recovered RF signal can be tuned by simply changing the bias voltage of the parent MZM (DC3). An erbium-doped fiber amplifier (EDFA) is used to compensate the insertion loss of the DPMZM and OBPF.

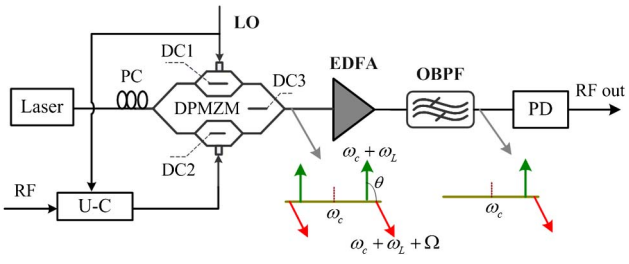

Fig. 1. Schematic of the proposed RF phase shifter. RF, radio frequency; LO, local microwave signal; DPMZM, dual parallel Mach–Zehnder modulator; PC, polarization controller; EDFA, erbium-doped fiber amplifier; U-C, electric up-converter; OBPF, optical bandpass filter.

Under small-signal modulation, only two first-order sidebands need to be considered. The optical field at the output of the DPMZM can be expressed as follows:

$$\begin{aligned} E_1(t) = A_1 &\left\{ \exp\left[j\left((\omega_c + \omega_L)t - \frac{\theta}{2} \right) \right] \right. \\ &\left. + \exp\left[j\left((\omega_c - \omega_L)t - \frac{\theta}{2} \right) \right] \right\} \\ &+ A_2 \left\{ \exp\left[j\left((\omega_c + \omega_L + \Omega)t + \frac{\theta}{2} \right) \right] \right. \\ &\left. + \exp\left[j\left((\omega_c - \omega_L - \Omega)t + \frac{\theta}{2} \right) \right] \right\}, \end{aligned} \tag{1}$$

where A_1 and A_2 are the amplitude of the first-order sidebands on the top and bottom arm, respectively; ω_c, ω_L, and Ω are the frequency of the optical carrier, local microwave and RF signal, respectively; θ is the relative phase difference between the two sidebands on the top and bottom arms, which can be express by

$$\theta = \pi V_3 / V_{\pi 3}, \tag{2}$$

where $V_{\pi 3}$ is the half-wave voltage of the parent MZM and V_3 is the bias voltage of the parent MZM (DC3).

Assuming that the two lower sidebands are suppressed by the OBPF, the optical field after the OBPF is given by

$$\begin{aligned} E_2(t) = &\sqrt{G}\sqrt{L_{\text{filter}}} A_1 \exp\left[j\left((\omega_c + \omega_L)t - \frac{\theta}{2} \right) \right] \\ &+ \sqrt{G}\sqrt{L_{\text{filter}}} A_2 \exp\left[j\left((\omega_c t + \omega_L + \Omega)t + \frac{\theta}{2} \right) \right], \end{aligned} \tag{3}$$

where G is the gain of the EDFA, and L_{filter} is the insertion loss of the optical filter. A phase-shifted RF current is produced by the beating of the two subcarriers during the photo-detection process, which can be described as

$$i(t) \propto E_2(t) \times E_2^*(t) = GL_{\text{filter}}A_1A_2\cos(\Omega t + \theta)$$
$$= GL_{\text{filter}}A_1A_2\cos(\Omega t + \pi V_3/V_{\pi 3}). \quad (4)$$

As can be seen from Eq. (4), the optical phase is introduced to the RF signal directly and one can easily control the phase shift of the RF signal linearly and continuously by tuning the bias voltage V_3.

It is worthwhile to mention that the performance of the proposed photonic RF phase shifter directly depends on the suppression ratio (SR) between the upper and lower sidebands. Nonlinear phase shift and power variation as phase shifting will occur when the lower sideband is not suppressed completely [13]. From Eq. (1), one can see that the frequency gap between the upper and lower sidebands can be adjusted by setting the frequency of the local microwave signal. The higher the frequency of the local microwave signal, the larger the frequency gap. Larger gap means the two sidebands are easily separated by the optical filters. In other words, the SR between the two sidebands after the optical filter can be improved by selecting the frequency of the local microwave signal. Theoretically, one of the two sidebands can be suppressed completely by the optical filter when the frequency of the local microwave signal is more than a half of the transition bandwidth of the optical filter, which is independent of the frequency of the under-phase-shifted RF signal (see the inset in Fig. 1). In contrast, to suppress one of the two sidebands, the frequency of the RF signal must be more than a half of the transition bandwidth of the optical filter for the single-drive scheme in [14].

In comparison with [14], the proposed scheme has three distinct advantages. (i) The effect of the extinction ratio of the modulator on the linearity and power variation as phase shifting is canceled since the generation of the phase-shifted RF signal is independent on the residual optical carrier. (ii) The instability induced by the slight drift between the optical carrier and central frequency of the optical filter is decreased owing to the fact that both of the two first-order upper sidebands are located in the passband of the optical filter where the amplitude response is flatter and the chromatic dispersion is smaller. (iii) The lowest frequency limit induced by the transition bandwidth of the optical filter can be overcome by setting the frequency of the local microwave signal more than a half of the transition bandwidth of the optical filter.

3. Experimental Results

The experimental setup is shown in Fig. 2. The optical carrier from a DFB laser with an optical power of 14 dBm is injected into a DPMZM (Photline, MXIQ-LN-40) with a usable bandwidth of 20 GHz. The bias voltage DC1 and DC2 of the DPMZM are biased at 9.4 and 9.3 V, respectively, corresponding to the minimum transmission points of the two

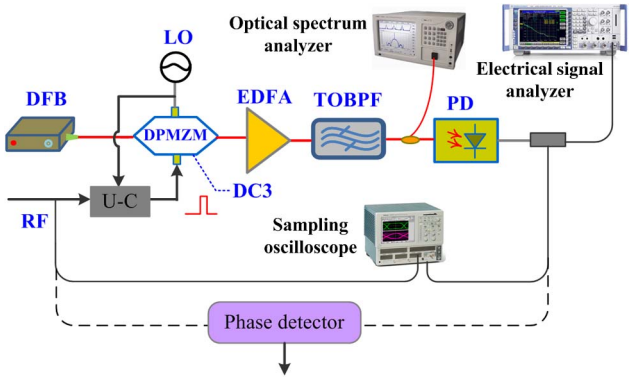

Fig. 2. Experimental setup of the proposed photonic RF phase shifter.

parallel sub-MZMs. The frequency of the local microwave signal is set at 9 GHz to ensure that the lower sideband can be suppressed completely by the consequent tunable OBPF (TOBPF, Alnair, BLV-200CL), which has a transition bandwidth about 16 GHz, a flatness of 0.2 dB and a chromatic dispersion of less than 0.4 ps/nm in the passband. The RF signal needed to be phase-shifted is set at 1 GHz and the U-C is realized by a microwave mixer and filter. A PD (Thorlabs, DEC010FC) with a bandwidth of 2.5 GHz is adopted to recover the phase-shifted RF signal. The phase shift is measured with a digital sampling oscillator (Tektronix, TDS8200) by comparing the RF signal recovered by the PD with the under-phase-shifted RF signal. An electrical signal analyzer (R&S, FUSP) is used to monitor the RF power variation. A microwave phase detector is used to observe the stability and phase tuning bandwidth of the phase shifter.

The optical spectrum after the TOBPF measured by a high resolution optical spectral analyzer (Apex, AP2040A) is shown in Fig. 3 when the lower (upper) sideband signal located in the stopband (passband) of the TOBPF. We can see that two lower sidebands are suppressed more than 45 dB compared to the upper sidebands. The influence of the lower sidebands can be ignored in this case according to the analysis in

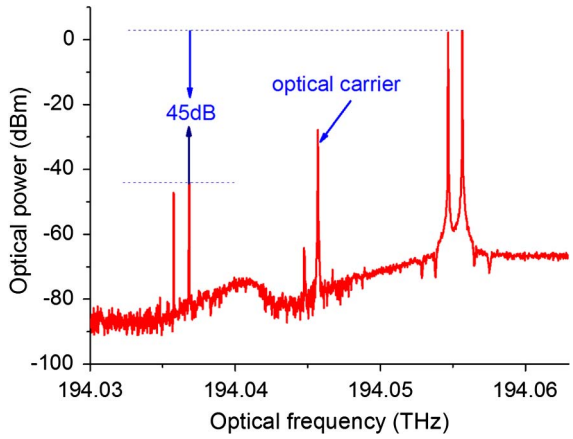

Fig. 3. Optical spectrum after TOBPF.

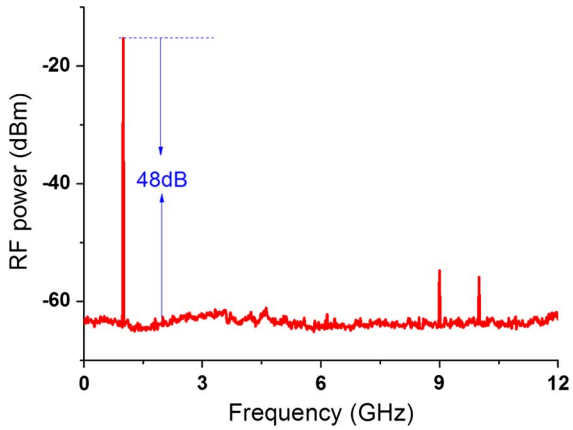

Fig. 4. Measured RF spectrum at the output of the PD.

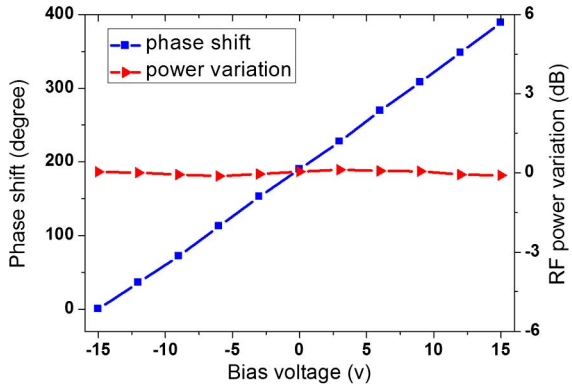

Fig. 6. Measured phase shift and power variation versus applied bias voltage of DC3.

[14]. We can also see that the optical carrier is not suppressed completely, which is mainly caused by the finite extinction ratio of the DPMZM. The residual optical carrier will induce unnecessary RF components by beating with the two upper sidebands, which can be suppressed further by selecting the optical filter with a narrow transition bandwidth or increasing the frequency of the local microwave signal to locate the optical carrier in the stopband.

The RF spectrum at the output of the PD measured by the electrical signal analyzer on the average mode is shown in Fig. 4. It can be seen that the recovered 1 GHz signal has a SNR of 48 dB under the resolution bandwidth of 1 MHz. The two high-frequency components (9 G and 10 GHz) from the beating of the residual optical carrier with two upper sidebands are almost completely suppressed by the limited bandwidth of the PD. Figure 5 shows the waveforms of the recovered 1 GHz RF signal when the bias voltage of the parent MZM (DC3) is set at 0, 6.9, and 13.7 V, which corresponds to the phase shift of 0°, 90°, and 180°, respectively. The measured phase shift and RF power variation are summarized in Fig. 6. We can see that a continuous and linear phase shift over 360° can be achieved when the bias voltage (DC3) is tuned from −15 to 15 V. The RF power variation as phase shifting is less than ±0.15 dB, which is preferable compared with the results in previous works [5,6,13].

Figure 7 shows the phase drift within 2000 s in an open laboratory environment when the bias voltage of DC3 keeps constant. The phase drift is less than 0.5°, which indicates the proposed phase shifter has a good short-term stability. It is noted that the long-term stability will be degraded with the fluctuation of environment temperature because the optical components and optical fiber are both sensitive to the temperature. An additional temperature control can be used to improve the long-term stability of the phase shifter.

The phase tuning bandwidth of the phase shifter is estimated by the pulse response method, which is realized by applying a pulse signal at the port of DC3 and measuring the rise time (from 10% to 90%) of the phase response signal captured by the phase detector. Figure 8 shows the pulse response signal when the DC3 is stimulated by a square signal at 100 kHz. We can see that the rise time (t_r) is 20 ns, which is mainly limited by the embedded RF block in the port of DC3. According to the well-known relation

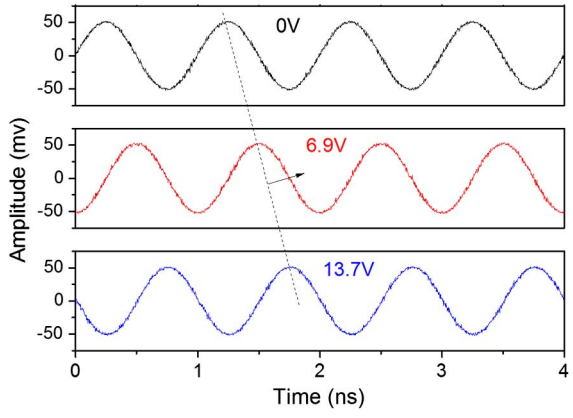

Fig. 5. Measured waveform at 1 GHz with phase shift of 0°, 90°, and 180°.

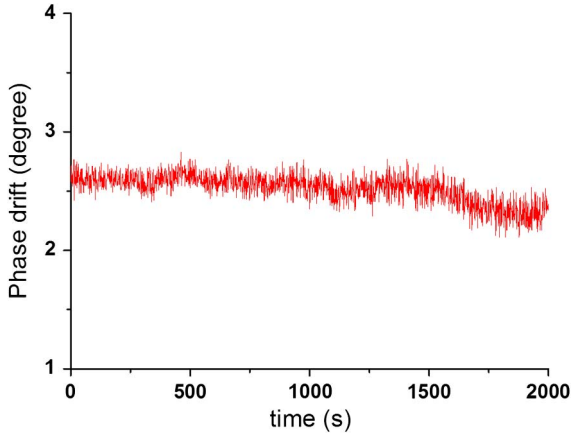

Fig. 7. Phase drift within 2000 s in an open laboratory environment.

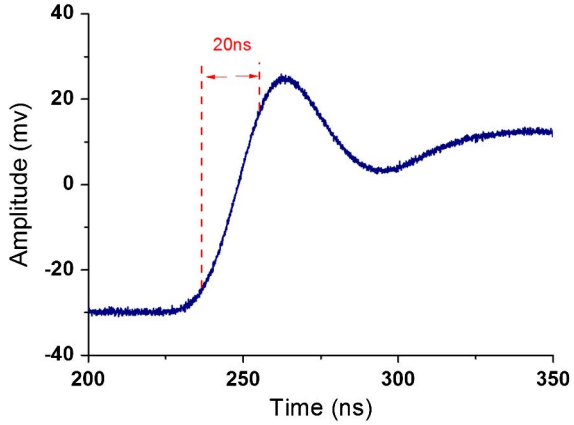

Fig. 8. Pulse response of the proposed photonic RF phase shifter.

[15], $B = 0.35/t_r$, the phase tuning bandwidth of the proposed phase shifter can reach 17 MHz, which is sufficient for many practical applications such as phased array beam-forming.

4. Conclusion

In this paper, we proposed and experimentally demonstrated a linear and stable photonic RF phase shifter based on a DPMZM and an optical filter using a two-drive scheme. A continuous and linear phase shift over 360° and power variation of less than ±0.15 dB at 1 GHz are achieved by tuning the bias voltage of the DPMZM from −15 to 15 V. The phase tuning bandwidth is up to 17 MHz and phase drift is less than 0.5° within 2000 s. Although the bandwidth of the proposed phase shifter may be limited by the electrical U-C, it can achieve a perfect performance in phase tunable range, linearity, and stability at the same time, which are difficult to realize with electrical phase shifters [16,17]. Moreover, the proposed phase shifter can also be regarded as a single sideband modulation transmitter, which provides a promising scheme to integrate the transmitter and phase compensator together in the applications like ultrastable frequency reference transfer via optical fiber [18,19].

Appendix A

Assuming that the input optical field of the DPMZM is $E_{\text{in}} \exp(j\omega_c t)$, the output optical fields from the sub-MZMs on the top arm and the bottom arm can be expressed as follows, respectively:

$$\begin{aligned} E_{\text{top}} &= \frac{1}{2\sqrt{2}} E_{\text{in}} \exp\left(j\omega_c t + j\frac{m_1}{2}\cos\omega_L t + j\frac{\varphi_1}{2}\right) \\ &\quad + \frac{1}{2\sqrt{2}} E_{\text{in}} \exp\left(j\omega_c t - j\frac{m_1}{2}\cos\omega_L t - j\frac{\varphi_1}{2}\right) \\ &= \frac{1}{\sqrt{2}} E_{\text{in}} \cos\left(\frac{m_1}{2}\cos\omega_L t + \frac{\varphi_1}{2}\right)\exp(j\omega_c t), \end{aligned} \tag{A1}$$

$$\begin{aligned} E_{\text{bot}} &= \frac{1}{2\sqrt{2}} E_{\text{in}} \exp\left[j\omega_c t + j\frac{m_2}{2}\cos(\omega_L+\Omega)t + j\frac{\varphi_2}{2}\right] \\ &\quad + \frac{1}{2\sqrt{2}} E_{\text{in}} \exp\left(j\omega_c t - j\frac{m_2}{2}\cos(\omega_L+\Omega)t - j\frac{\varphi_2}{2}\right) \\ &= \frac{1}{\sqrt{2}} E_{\text{in}} \cos\left[\frac{m_2}{2}\cos(\omega_L+\Omega)t - \frac{\varphi_2}{2}\right]\exp(j\omega_c t), \end{aligned} \tag{A2}$$

where $\varphi_i = \pi V_i / V_{\pi\text{DC}}$ $(i = 1,\ 2)$, $m_1 = \pi V_L / V_{\pi\text{RF}}$, $m_2 = \pi V_{\text{UC}} / V_{\pi\text{RF}}$, V_i is the bias voltage of sub-MZMs on the top and bottom arm, $V_{\pi\text{RF}}$ and $V_{\pi\text{DC}}$ is the RF half-wave voltage and DC half-wave voltage of the sub-MZM (assuming that the two sub-MZMs are symmetrical), V_L and V_{UC} are the amplitudes of the local microwave signal and the up-converted signal, respectively.

The optical field at the output of the parent-MZM can be derived by combining the above optical signals from the two sub-MZMs:

$$\begin{aligned} E_{\text{out}} &= \frac{1}{\sqrt{2}}\left[E_{\text{top}} \exp\left(-j\frac{\theta}{2}\right) + E_{\text{bot}} \exp\left(j\frac{\theta}{2}\right)\right] \\ &= \frac{1}{4} E_{\text{in}} \left\{\cos\left[\frac{m_1}{2}\cos\omega_L t + \frac{\varphi_1}{2}\right]\exp\left(-j\frac{\theta}{2}\right) \right. \\ &\quad \left. + \cos\left[\frac{m_2}{2}\cos(\omega_L+\Omega)t + \frac{\varphi_2}{2}\right]\exp\left(j\frac{\theta}{2}\right)\right\}, \end{aligned} \tag{A3}$$

where $\theta = \pi V_3 / V_{\pi 3}$, $V_{\pi 3}$ is the half-wave voltage of the parent MZM, and V_3 is the bias voltage of the parent MZM.

When two sub-MZMs are biased at null point, the output optical field of the DPMZM under small signal modulation can be simplified as

$$\begin{aligned} E_{\text{out}} &= \frac{1}{2} E_{\text{in}} J_1(m_1/2)\left\{\exp\left[j\left((\omega_c+\omega_L)t - \frac{\theta}{2}\right)\right] \right. \\ &\quad \left. + \exp\left[j\left((\omega_c-\omega_L)t - \frac{\theta}{2}\right)\right]\right\}\exp(j\pi) \\ &\quad + \frac{1}{2} E_{\text{in}} J_1(m_2/2)\left\{\exp\left[j\left((\omega_c+\omega_L+\Omega)t + \frac{\theta}{2}\right)\right] \right. \\ &\quad \left. + \exp\left[j\left((\omega_c t-\omega_L-\Omega)t + \frac{\theta}{2}\right)\right]\right\}\exp(j\pi), \end{aligned} \tag{A4}$$

where $J_1(\cdot)$ is the first-order Bessel function of the first kind.

This work was supported in part by the 973 Program (2011CB301700), the National Natural Science Foundation of China (61071011, 61127016, and 61107041), the International Cooperation Project from the Ministry of Science and Technology of China (2011FDA11780), Shanghai Pujiang Program (12PJ1405600), Shanghai Excellent Academic Leader Program (12XD1406400), and Zhejiang Provincial Nature Science Foundation (LY12F05002).

References

1. R. A. Minasian, "Optical signal processing of microwave signals," IEEE Trans. Microw. Theory Tech. **54**, 832–846 (2006).
2. J. Capmany, B. Ortega, and D. Pastor, "Tutorial on microwave photonic filters," J. Lightwave Technol. **24**, 201–229 (2006).
3. Y. Yu and J. P. Yao, "A tunable microwave photonic filter with a complex coefficient using an optical RF phase shifter," IEEE Photon. Technol. Lett. **24**, 201–209 (2006).
4. X. X. Xue, X. P. Zheng, H. Y. Zhang, and B. K. Zhou, "Tunable 360° photonic radio frequency phase shifter based on optical quadrature double-sideband modulation and differential detection," Opt. Lett. **36**, 4641–4643 (2011).
5. E. H. W. Chan, W. W. Zhang, and R. A. Minasian, "Photonic RF phase shifter based on optical carrier and RF modulation sidebands amplitude and phase control," J. Lightwave Technol. **30**, 3672–3678 (2012).
6. S. S. Lee, A. H. Udupa, H. Erlig, H. Zhang, Y. Chang, C. Zhang, D. H. Chang, D. Bhattacharya, B. Tsap, and H. R. Fetterman, "Demonstration of a photonically controlled RF phase shifter," IEEE Microw. Guided Wave Lett. **9**, 357–359 (1999).
7. X. Sun, S. Fu, K. Xu, J. Zhou, P. Shum, J. Yin, X. Hong, J. Wu, and J. Lin, "Photonic RF phase shifter based on a vector-sum technique using stimulated Brillouin scattering in dispersion shifted fiber," IEEE Trans. Microw. Theory Tech. **58**, 3206–3212 (2010).
8. A. Loayssa and F. J. Lahoz, "Broad-band RF photonic phase shifter based on stimulated Brillouin scattering and single-sideband modulation," IEEE Photon. Technol. Lett. **18**, 357–359 (2006).
9. J. Sancho, J. Lloret, I. Gaslla, S. Sales, and J. Capmany, "Fully tunable 360° microwave photonic phase shifter based on a single semiconductor optical amplifier," Opt. Express **19**, 17421–17426 (2011).
10. Y. Dong, H. He, and W. S. Hu, "Photonic microwave phase shifter/modulator based on a nonlinear optical loop mirror incorporating a Mach–Zehnder interferometer," Opt. Lett. **32**, 745–747 (2007).
11. H. Chen, Y. Dong, H. He, W. S. Hu, and L. M. Zhang, "Photonic radio-frequency phase shifter based on polarization interference," Opt. Lett. **34**, 2375–2377 (2009).
12. Z. H. Li, C. Y. Yu, Y. Dong, and L. H. Cheng, "Linear photonic radio frequency phase shifter using a different-group-delay element and an optical phase modulator," Opt. Lett. **35**, 1881–1883 (2010).
13. S. L. Pan and Y. M. Zhang, "Tunable and wideband microwave photonic phase shifter based on a single-sideband polarization modulator and a polarizer," Opt. Lett. **37**, 4483–4485 (2012).
14. J. G. Shen, G. L. Wu, W. Zou, and J. P. Chen, "A photonic RF phase shifter based on a dual-parallel Mach–Zehnder modulator and an optical filter," Appl. Phys. Express **5**, 072502 (2012).
15. E. Bogatin, *Signal Integrity—Simplified* (Academic, 2003).
16. H. Kim, A. B. Kozyrev, A. Karbassi, and D. W. Van, "Linear tunable phase shifter using a left-handed transmission line," IEEE Microw. Wirel. Compon. Lett. **15**, 366–368 (2005).
17. Y. Park, "A CMOS voltage controlled continuous phase shifter with active loss compensation," IEEE Microw. Wirel. Compon. Lett. **22**, 421–423 (2012).
18. S. M. Forma, K. W. Holman, D. D. Hudson, D. J. Jones, and J. Ye, "Remote transfer of ultrastable frequency references via fiber networks," Rev. Sci. Instrum. **78**, 021101 (2007).
19. L. M. Zhang, L. Chang, Y. Dong, W. L. Xie, H. He, and W. S. Hu, "Phase drift cancellation of remote radio frequency transfer using an optoelectronic delay-locked loop," Opt. Lett. **36**, 873–875 (2011).